Biochimica et Biophysica Acta xxx (2016) xxx–xxx

Contents lists available at ScienceDirect

Biochimica et Biophysica Acta

journal homepage: www.elsevier.com/locate/bbagen

A long-linker conjugate of fluorescein and triphenylphosphonium as mitochondria-targeted uncoupler and fluorescent neuro- and nephroprotector

Yuri N. Antonenko [a,*], Stepan S. Denisov [a,b], Denis N. Silachev [a], Ljudmila S. Khailova [a], Stanislovas S. Jankauskas [a], Tatyana I. Rokitskaya [a], Tatyana I. Danilina [a], Elena A. Kotova [a], Galina A. Korshunova [a], Egor Y. Plotnikov [a], Dmitry B. Zorov [a]

[a] Belozersky Institute of Physico-Chemical Biology, Lomonosov Moscow State University, Moscow 119991, Russia
[b] Faculty of Chemistry, Lomonosov Moscow State University, Moscow 119991, Russia

ARTICLE INFO

Article history:
Received 22 April 2016
Received in revised form 16 June 2016
Accepted 16 July 2016
Available online xxxx

Keywords:
Mitochondria
Mild uncoupler
Protonophore
Fluorescein
Membrane potential

ABSTRACT

Background: Limited uncoupling of oxidative phosphorylation is known to be beneficial in various laboratory models of diseases. Linking a triphenyl-phosphonium cation to fluorescein through a decyl (C_{10}) spacer yields a fluorescent uncoupler, coined mitoFluo, that selectively accumulates in energized mitochondria (Denisov et al., Chem.Commun. 2014).
Methods: Proton-transport activity of mitoFluo was tested in liposomes reconstituted with bacteriorhodopsin. To examine the uncoupling action on mitochondria, we monitored mitochondrial membrane potential in parallel with oxygen consumption. Neuro- and nephroprotecting activity was detected by a limb-placing test and a kidney ischemia/reperfusion protocol, respectively.
Results: We compared mitoFluo properties with those of its newly synthesized analog having a short (butyl) spacer (C_4-mitoFluo). MitoFluo, but not C_4-mitoFluo, caused collapse of mitochondrial membrane potential resulting in stimulation of mitochondrial respiration. The dramatic difference in the uncoupling activity of mitoFluo and C_4-mitoFluo was in line with the difference in their protonophoric activity on a lipid membrane. The accumulation of mitoFluo in mitochondria was more pronounced than that of C_4-mitoFluo. MitoFluo decreased the rate of ROS production in mitochondria. MitoFluo was effective in preventing consequences of brain trauma in rats: it suppressed trauma-induced brain swelling and reduced a neurological deficit. Besides, mitoFluo attenuated acute kidney injury after ischemia/reperfusion in rats.
Conclusions: A long alkyl linker was proved mandatory for mitoFluo to be a mitochondria- targeted uncoupler. MitoFluo showed high protective efficacy in certain models of oxidative stress-related diseases.
General significance: MitoFluo is a candidate for developing therapeutic and fluorescence imaging agents to treat brain and kidney pathologies.

1. Introduction

Uncouplers of oxidative phosphorylation of protonophoric type dissipate the electrochemical potential of hydrogen ions ($\Delta\bar{\mu}_{H^+}$) on the inner mitochondrial membrane which is known to couple respiratory pumps with ATP synthesis. The most popular uncoupler 2,4-dinitrophenol (DNP) was used to fight obesity at the beginning of the 20th century [1]. Recently, DNP and other uncouplers have been shown to exert effective protection in diabetic models in mice and rats [2–4], besides they display neuroprotective and cardioprotective activities in different models [5]. Since mitochondria is a major source of reactive oxygen species (ROS) playing important role in the development of oxidative stress-related pathologies [6–8], the beneficial action of uncouplers

Abbreviations: $\Delta\psi$, transmembrane electric potential difference; BLM, bilayer lipid membrane; DPhPC, diphytanoylphosphatidylcholine; C_4R1, rhodamine 19 *n*-butyl ester; mitoFluo (or C_{10}-mitoFluo), 10-[2-(3-hydroxy-6-oxo-xanthen-9-yl)benzoyl]oxydecyl-triphenyl-phosphonium bromide; C_4-mitoFluo, 4-[2-(3-hydroxy-6-oxo-xanthen-9-yl)benzoyl]oxybutyl-triphenyl-phosphonium bromide; C_8-FL, fluorescein *n*-octyl ester; Amplex Red, N-acetyl-3,7-dihydroxyphenoxazine; TMRE, tetramethylrhodamine ethyl ester; CCCP, carbonyl cyanide *m*-chlorophenylhydrazone; DNP, 2,4-dinitrophenol; MitoDNP, 3-(3,5-dinitro-4-hydroxyphenyl)propyltriphenylphosphonium methanesulfonate; FCCP, carbonyl cyanide-*p*-trifluoromethoxyphenylhydrazone; DiS-C3-(5), 3,3′-dipropylthiodicarbocyanine iodide; BHT, butylated hydroxytoluene; HRP, horseradish peroxidase; FCS, fluorescence correlation spectroscopy; MR, magnetic resonance; MRI, magnetic resonance imaging; PBS, phosphate buffered saline; PIA, peak intensity analysis; ROS, reactive oxygen species; I/R, ischemia/reperfusion; TBI, traumatic brain injury; BUN, blood urea nitrogen; i/n, intranasal.

* Corresponding author at: Belozersky Institute of Physico-Chemical Biology, Moscow State University, Moscow 119991, Russia.
E-mail address: antonen@genebee.msu.ru (Y.N. Antonenko).

http://dx.doi.org/10.1016/j.bbagen.2016.07.014
0304-4165/

could be related to the steep dependence of the ROS generation on $\Delta\overline{\mu}_{H^+}$ [9,10]. Of relevance to this point, it has been hypothesized that one of the key functions of mitochondrial uncoupling proteins (UCPs) is to lower the mitochondrial membrane potential if it exceeds a certain threshold, thus regulating ROS production [11,12].

High concentrations of uncouplers exert deleterious action obviously through the impairment of mitochondrial energetics and a drop in ATP concentration. In fact, uncouplers are used as pesticides [13] and are promising candidates for antibiotics [14]. Unfortunately, overdosage of DNP caused several deaths in humans prior to the ban of its use as a drug [15]. Thus, it is of importance to find a "mild uncoupler" having a broad window between concentrations starting to decrease the membrane potential and concentrations blocking ATP synthesis. The well-known antioxidant butylated hydroxytoluene (BHT) has been found to exhibit the uncoupling activity with the broad concentration window [16]. However, BHT is unable to fully stimulate mitochondrial respiration even at high concentrations. Besides, it is unknown whether BHT is able to fight obesity similar to DNP or the other frequently used uncoupler usnic acid [17,18].

The toxic action of uncouplers is generally assumed to result from critical depolarization of the inner mitochondrial membrane leading to complete uncoupling of oxidative phosphorylation. However, this important issue has not been confirmed in direct experiments. Moreover, poor correlation has been observed between the effect of DNP and its derivatives on the respiration of isolated mitochondria and the toxic action on mice [13]. In particular, LD50 for toxicity of DNP and 6-cyclohexyl-DNP differs 1.5-fold, while uncoupling concentrations differ more than 30-fold. The data on the inhibition of the growth of yeast cells by DNP and FCCP support the idea of non-mitochondrial toxicity of these conventional uncouplers [19]. The possible non-mitochondrial target of uncouplers could be the cytoplasmic membrane potential [20,21]. Besides, DNP has been found to bind to several important non-mitochondrial proteins [22,23]. FCCP has been shown to be susceptible to the attack of sulfhydryl reagents [24] pointing to a possibility of the interaction with cystein residues of cytoplasmic or membrane proteins [25].

This consideration suggests that toxic action of uncouplers can be diminished by affecting their pharmacokinetics. In fact, it has been shown that the use of DNP methyl ester instead of DNP improves the therapeutic action of the uncoupler in diabetic models in mice [26]. Besides, DNP incorporated in nanoparticles has appeared to effectively ameliorate hypertriglyceridemia, insulin resistance, hepatic steatosis, and diabetes in rats [2]. In line with these findings, the design of mitochondria-targeted uncouplers may dramatically reduce the side effects because of their selective accumulation in mitochondria. Unfortunately, conjugation of the mitochondrial cationic tag triphenylphosphonium (TPP) to DNP (MitoDNP) has produced an inactive uncoupler probably due to inhibition of the efflux of deprotonated MitoDNP [27]. On the other hand, conjugation of TPP to certain polyphenols led to compounds exhibiting uncoupling action on isolated mitochondria [28]. It has been shown recently in our laboratory that the cationic compound rhodamine 19 *n*-dodecyl ester (C_{12}R1) accumulates in mitochondria and uncouples oxidative phosphorylation [29]. More hydrophilic rhodamine 19 *n*-butyl ester (C_4R1) is even more effective in mitochondria, although its protonophoric action on artificial membranes is weaker than that of C_{12}R1 [30]. According to [30], this paradox can be explained by involvement of certain mitochondrial proteins in the uncoupling action of C_4R1. Importantly, C_4R1 has been used successfully for combating obesity in mice at concentrations less than those of DNP [31].

In our previous work [32], we have synthesized and tested a conjugate of TPP with a derivative of fluorescein, which exhibits the uncoupling action of the protonophoric type (mitoFluo or C_{10}-mitoFluo, structure shown in Fig. 1). Importantly, it accumulates in isolated mitochondria upon their energization. Besides,

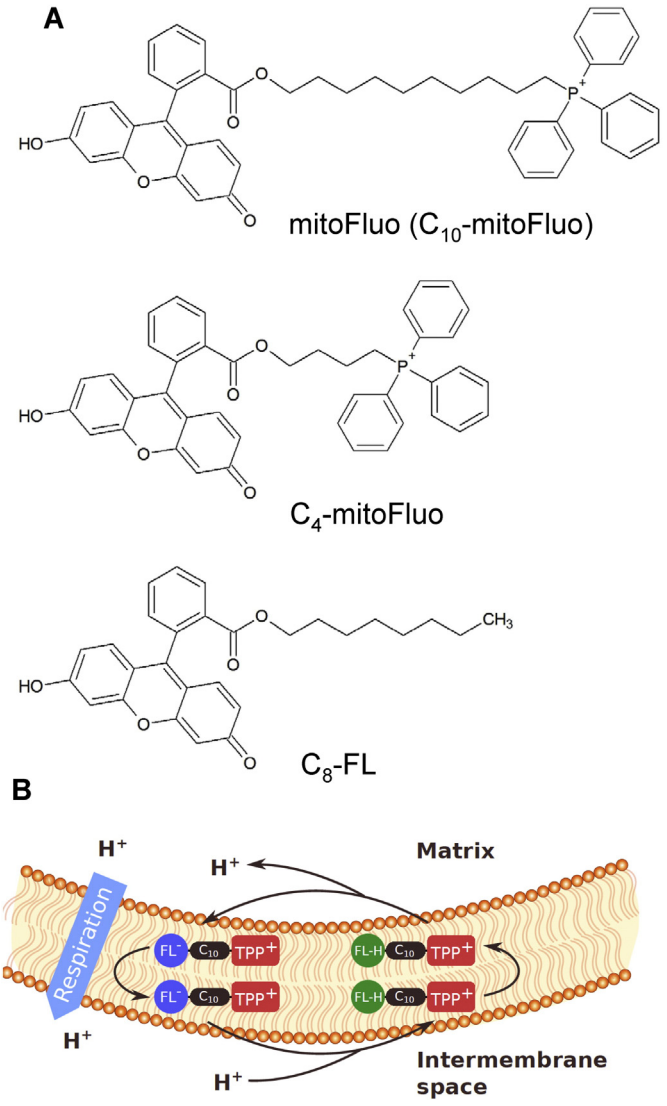

Fig. 1. A. Chemical structures of mitoFluo (10-[2-(3-hydroxy-6-oxo-xanthen-9-yl)benzoyl]oxydecyl-triphenyl-phosphonium bromide, or C_{10}-mitoFluo), C_4-mitoFluo (4-[2-(3-hydroxy-6-oxo-xanthen-9-yl)benzoyl]oxybutyl-triphenyl-phosphonium bromide), and C_8-FL (fluorescein *n*-octyl ester). **B.** Scheme of mitoFluo-mediated proton transport through the inner mitochondrial membrane.

1 μM of mitoFluo stimulates mitochondrial respiration similar to FCCP, thus exhibiting properties of a true uncoupler. These results prompted us to conduct further research on the properties of this interesting compound displaying bright fluorescence in mitochondria and liposomes. The present study, aimed at elucidating tissue-protective mechanisms of the mitochondria-specific protonophore mitoFluo, i) addressed structural requirements for mitochondria-specific uncoupling (structure-activity relationship between mitoFluo and its two analogues: C_4-mitoFluo, having a short linker between fluorescein and the cationic TPP group, and C_8-FL, lacking a TPP moiety (Fig. 1) [33]) and ii) directly demonstrated protective effects on animal tissue following acute injury. In contrast to mitoFluo, the more hydrophilic C_4-mitoFluo neither caused dissipation of mitochondrial membrane potential, nor stimulated mitochondria respiration. Moreover, the short-linker conjugate exhibited poor accumulation in mitochondria upon energization. Importantly, mitoFluo exhibited neuroprotective and nephroprotective action on the models of brain trauma and kidney ischemia/reperfusion in rats.

Please cite this article as: Y.N. Antonenko, et al., A long-linker conjugate of fluorescein and triphenylphosphonium as mitochondria-targeted uncoupler and fluorescent neuro- and neph..., Biochim. Biophys. Acta (2016), http://dx.doi.org/10.1016/j.bbagen.2016.07.014

2. Materials and methods

2.1. Materials

MitoFluo and C_8-FL were synthesized as described in [32,33]. Sucrose was from ICN. Rhodamine 6G was from Fluka. Tetramethylrhodamine ethyl ester (TMRE), and Amplex Red reagent were from Invitrogen. Total *E. coli* lipid was from Avanti Polar Lipids. Other chemicals were from Sigma-Aldrich.

2.2. Synthesis of 4-brombutyl-triphenyl-phosphonium bromide

The synthesis was similar to that described in [32]. Namely, a solution of 1,4-dibrombutyl (1.1 ml, 12 mmol) and triphenylphosphine (2.62 g, 10 mmol) in benzene (0.5 ml) was heated at 80 °C during 20 h in a tightly closed flask. Then the reaction mass was cooled to 20 °C, diluted with dichloromethane and evaporated to dryness. The residue was dissolved in a minimal volume of dichloromethane, then an excess of diethyl ester was added and the suspension formed was kept at 4 °C until the solution became clear. Then the liquid phase was decanted, the residue was dissolved again in dichloromethane and treated with diethyl ether to complete precipitation. This procedure was repeated three times. Finally the residue was dissolved in a minimal volume of the solvent system ethanol-dichloromethane (1:5) and applied to a chromatographic silica gel column (MN Kieselgel 60, 240–400 mesh) in the same solvent system as an eluent. Detection was carried out using TLC by UV-absorbance and Dragendorf reaction. Fractions with the same chromatographic mobilities were combined and evaporated in vacuo (yield 1,8 g, 40%). ESI-MS: calculated for $C_{22}H_{23}PBr$ 398.3, observed 399.2 $(M + H)^+$.

2.3. Synthesis of 4-[2-(3-hydroxy-6-oxo-xanthen-9-yl)benzoyl]oxybutyl-triphenyl-phosphonium bromide (C_4-mitoFluo)

A solution of fluorescein (1 g, 3.0 mmol) and sodium carbonate (0.5 g) in DMF (50 ml) was heated to 60 °C. The solution of 1,4-brombutyltriphenylphosphonium bromide (1 g, 2.2 mmol) in a minimal volume of dichloromethane was added dropwise and the reaction was carried out for 3 h under stirring at 60 °C. Then the reaction mass was cooled and diluted with 100 ml of dichloromethane. The organic solution was washed twice with 5% hydrochloric acid and dried over calcium chloride. The organic phase was filtered and evaporated in vacuo. The residue was dissolved in a minimal volume of the solvent mixture ethanol-dichloromethane (1:5) and applied to a silica gel column (MN Kieselgel 60, 240–400 mesh) in the same solvent system used as an eluent for chromatographic purification. Fractions were detected by direct visualization of colored zones and additionally analyzed using TLC, those having equal chromatographic mobilities were combined. The solvents were removed and the residues were dried in vacuo and analyzed by LC-MS. The resulting compound was eluted as an orange band and after evaporation of solvents was obtained as orange powder (320 mg, 20%). ESI-MS: calculated for $C_{42}H_{34}O_5P$ 649.6; observed 649.4.

2.4. Planar phospholipid bilayers

Bilayer lipid membrane (BLM) was formed from 2% decane solution of *E. coli* total lipid on a 0.6-mm aperture in a Teflon septum separating the experimental chamber into two compartments of equal size (volumes, 3 ml). Electrical parameters were measured with two AgCl electrodes placed into the solutions on the two sides of the BLM via agar bridges, using a Keithley 6517 amplifier (Cleveland, Ohio, USA). The incubation mixture contained 10 mM MES, 10 mM β-alanine, 100 mM KCl, pH 4.

2.5. Proton transport in liposomes reconstituted with bacteriorhodopsin

Bacteriorhodopsin (bR), isolated from *Halobacterium salinarum* cells, was a generous gift of Dr. Sergey Sychev (Shemyakin and Ovchinnikov Institute of Bioorganic Chemistry, Moscow). The reconstitution of bR into proteoliposomes containing Type II-S phospholipid from soybean (Sigma-Aldrich) was performed as described in [34]. 10 μl of proteoliposome dispersion (0.25 mg/ml of bR) was added to 1 ml of 150 mM KCl, 10 mM Tris, 10 mM MES, 10 μM oxonol VI, and pH was adjusted to 7.4. The measurements were conducted in the thermostated cell at 15 °C with a Panorama Fluorat 02 spectrofluorimeter (Lumex, Russia) adjusting excitation at 590 nm and emission at 620 nm.

2.6. Isolation of rat liver mitochondria

Rat liver mitochondria (RLM) were isolated by differential centrifugation [35] in medium containing 250 mM sucrose, 5 mM MOPS, 1 mM EGTA, and bovine serum albumin (0.5 mg/ml), pH 7.4. The final washing was performed in medium of the same composition. Protein concentration was determined using the Biuret method. Handling of animals and experimental procedures with them were conducted in accordance with the international guidelines for animal care and use and were approved by the Institutional Ethics Committee of Belozersky Institute of Physico-Chemical Biology at Moscow State University.

2.7. Mitochondrial respiration

Respiration of isolated mitochondria was measured using a standard polarographic technique with a Clark-type oxygen electrode (Strathkelvin Instruments, UK) at 25 °C using the 782 system software. The incubation medium contained 250 mM sucrose, 5 mM MOPS, and 1 mM EGTA, pH 7.4. The mitochondrial protein concentration was 0.8 mg/ml. Oxygen uptake was expressed as nmol/min·mg protein.

2.8. Membrane potential ($\Delta\Psi$) measurement in isolated mitochondria

$\Delta\Psi$ was estimated using the safranine O dye [36]. The difference in the absorbance between at 555 and 523 nm (ΔA) was recorded with an Aminco DW-2000 spectrophotometer in the dual wavelength mode. The following incubation medium was used: 250 mM sucrose, 5 mM MOPS, 1 mM EGTA, 2 μM rotenone, 5 mM succinate (pH 7.4), 15 μM safranine O. The mitochondrial protein content was 0.6–0.9 mg protein/ml, the temperature was 26 °C.

2.9. Mitochondrial ROS measurements by Amplex Red fluorescence assay

Hydrogen peroxide production was measured fluorometrically employing the dye Amplex Red (Molecular Probes, Eugene, OR, USA) in combination with horseradish peroxidase (HRP) [37]. In these experiments, the incubation medium was supplemented with 1 μM Amplex Red reagent and 5 U/ml HRP. Amplex Red (N-acetyl-3,7-dihydroxyphenoxazine) is a non-fluorescent molecule that when oxidized by H_2O_2 in the presence of HRP produces resorufin, a highly fluorescent compound with an emission peak at about 585 nm. The detection of H_2O_2 in mitochondrial suspensions was recorded as an increase in fluorescence at 585 nm with the excitation wavelength set at 550 nm. The fluorescence response was calibrated by sequential additions of known amounts of hydrogen peroxide solution.

2.10. FCS experimental setup

Uptake of fluorescein derivatives by isolated mitochondria was measured by fluorescence correlation spectroscopy (FCS). Peak intensity analysis (PIA) was applied to fluorescence time traces of suspensions of dye-doped mitochondria, representing sequences of peaks of different intensity, which reflected their random walk through the confocal

Please cite this article as: Y.N. Antonenko, et al., A long-linker conjugate of fluorescein and triphenylphosphonium as mitochondria-targeted uncoupler and fluorescent neuro- and neph..., Biochim. Biophys. Acta (2016), http://dx.doi.org/10.1016/j.bbagen.2016.07.014

volume [38]. The experimental data were obtained under stirring, which increased the number of events by about three orders of magnitude, thus substantially enhancing the resolution of the method. The setup of our own construction was described previously [38]. Briefly, fluorescence excitation and detection were provided by a Nd:YAG solid state laser with a 532-nm beam, attached to an Olympus IMT-2 epifluorescence inverted microscope equipped with a 40×, NA 1.2 water immersion objective (Carl Zeiss, Jena, Germany). The fluorescence passed through an appropriate dichroic beam splitter and a long-pass filter and was imaged onto a 50-μm core fiber coupled to an avalanche photodiode (SPCM-AQR-13-FC, Perkin Elmer Optoelectronics, Vaudreuil, Quebec, Canada). The output signal $F(t)$ was sent to a personal computer, using a fast interface card (Flex02-01D/C, Correlator.com, Bridgewater, NJ). The signal was measured in Hz, i.e. number of photons per second. The data acquisition time T was 30 s. The card generated the autocorrelation function of the signal $G(\tau)$ defined as

$$G(\tau) = \frac{1}{T}\int_0^T F(t)F(t+\tau)dt = <F(t+\tau)F(t)>$$

2.11. Traumatic brain injury model (TBI)

The animal protocols used in this work were evaluated and approved by the institutional animal ethics committee in accordance with FELASA guidelines. The experiments were performed on outbred white male rats (350–400 g). The animals had unlimited access to food and water and were kept in cages with a temperature controlled environment (20 ± 2 °C) with light on from 9 AM to 9 PM. For all surgical procedures rats were anesthetized with i/p injections of 300 mg/kg (12%) chloral hydrate. A feedback-controlled heating pad maintained the core temperature (37.0 ± 0.5 °C) during ischemia supplemented with an infrared lamp until awake.

In the present work, we employed our own modification of the earlier used model of focal open severe brain trauma in rats [39,40]. To create the trauma, the left frontal part of the skull was trepanized above the sensorimotor cortex zone, and a movable Teflon piston 4 mm in diameter with depth of insertion of 2.5 mm was placed into it; this piston was struck from the height of 10 cm with a 50 g load sliding along a directing rail. For localization of the sensorimotor cortex zone we used following stereotaxic coordinates; +4 to −3 mm anterior and posterior from bregma and +1 to +4.5 mm lateral from the midline. In sham-operated rats, the experiments have been done using the same protocol except that trauma was excluded. The rats were treated by intranasal (i/n) administration of mitoFluo immediately after induction of TBI. Saline (40 μl) containing mitoFluo at a dose 500 nmol/kg was administered i/n as drops released from a small pipette every 5 min into both sides of the nasal cavity, followed by 5 μl for the last dose (for a total of 20 min). Rats were randomly divided in 3 groups as follows: (1) Sham + Saline (n = 10), (2) TBI + Saline (n = 10), (3) TBI + mitoFluo (n = 11). Volume of the damage was quantified by analyzing brain magnetic resonance (MR)-images obtained 14 day after the TBI as described previously [41].

2.12. Limb-placing test

A modified version of the limb-placing test, consisting of seven tasks, was used to assess forelimb and hindlimb responses to tactile and proprioceptive stimulation [42]. The rats were habituated for handling and tested before operation and at 1st, 2nd, 4th, 7th and 14th post-injury days. For each task, the following scores were used: 2 points, normal response; 1 point, delayed and/or incomplete response; 0 points, no response. The total score over seven tasks was evaluated.

2.13. Kidney ischemia/reperfusion (I/R) protocol

Rats were randomly divided by 3 groups as follows: Sham + Saline (n = 5), I/R + Saline (n = 8), I/R + mitoFluo (n = 5). Rats in "Sham + Saline" group were subjected to the right side nephrectomy. In "I/R + Saline" group animals were subjected to 40-min warm ischemia of the left kidney and right side nephrectomy. In "I/R + mitoFluo" animals were treated with mitoFluo in addition to left kidney I/R and right kidney removal. Briefly, unilateral renal arteries were clamped by a microvascular clip for 40 min, and then circulation was restored by removing the clip. During operation, the body temperature of the rat was maintained at 37 ± 0.5 °C. On the second day after ischemia blood samples were taken to determine blood urea nitrogen (BUN). The therapeutic protocol of mitoFluo treatment: i/p injection of 500 nmoles/kg mitoFluo 3 h before I/R, 1 h after I/R, and subsequent injections at 13, 25 and 37 h; in total, each animal received 2500 nmoles/kg mitoFluo.

2.14. Analysis of mitoFluo accumulation in kidney

Rats were injected i/p with 2 μmol/kg mitoFluo, kidneys were excised after 3 h and sliced using a VibroSlice microtome (World Precision Instruments, USA) into 100 mm thick sections. Slices were imaged with a LSM510 inverted confocal microscope (Carl Zeiss Inc, Jena, Germany) with excitation at 488 nm and emission collected at 505–530 nm. As a negative control kidneys from untreated animals were used.

2.15. Statistics

Statistical analyses were performed using STATISTICA 7.0 for Windows (StatSoft, Inc.). All data are presented as means ± standard error of means (SEM). The neurological deficit scores are expressed as median ± interquartile ranges, the 25th to 75th percentile being shown in parentheses. Variance homogeneity was assessed with Levene's test. Statistical differences between groups in the data of brain damage volume and brain swelling were analyzed using one-way ANOVA with Tukey's post-hoc test. Statistical differences in the limb-placing tests between groups were analyzed using the Kruskal–Wallis test with the Mann–Whitney U-test (the Bonferroni post-hoc correction was applied). Values for $p < 0.05$ were assumed to be statistically significant.

3. Results and discussion

To study the uncoupling activity of mitoFluo and C_4-mitoFluo, we measured the mitochondrial membrane potential (the electrical potential difference across the inner mitochondrial membrane) via the absorbance changes of safranine O. As seen in Fig. 2A, the addition of mitoFluo to energized mitochondria led to a drop in the mitochondrial membrane potential, which was enhanced with increasing the mitoFluo concentration (black curve). On the contrary, no decrease in the membrane potential was observed upon the addition of the short-linker conjugate C_4-mitoFluo (red curve). Another fluorescein analog lacking the TPP group, C_8-FL, decreased the membrane potential at concentrations similar to those of mitoFluo (blue curve). Absorbance measurements in control experiments without safranine showed that the additions of mitoFluo and C_4-mitoFluo did not contribute to the absorbance at 555 nm and 523 nm measured in the presence of 10 μM safranine (data not shown). The inability of C_4-mitoFluo to uncouple mitochondria also manifested itself in the failure of this compound to increase the respiration rate, in contrast to the marked acceleration of mitochondrial respiration by mitoFluo (insert in Fig. 2A, see also [32]).

These results were further supported by comparing effects of mitoFluo and C_4-mitoFluo on the light-induced generation of membrane potential on liposomal membranes with reconstituted bacteriorhodopsin, as measured by oxonol VI fluorescence. It is seen in Fig. 2B that the oxonol response to illumination with green light (marked ON) was substantially

Please cite this article as: Y.N. Antonenko, et al., A long-linker conjugate of fluorescein and triphenylphosphonium as mitochondria-targeted uncoupler and fluorescent neuro- and neph..., Biochim. Biophys. Acta (2016), http://dx.doi.org/10.1016/j.bbagen.2016.07.014

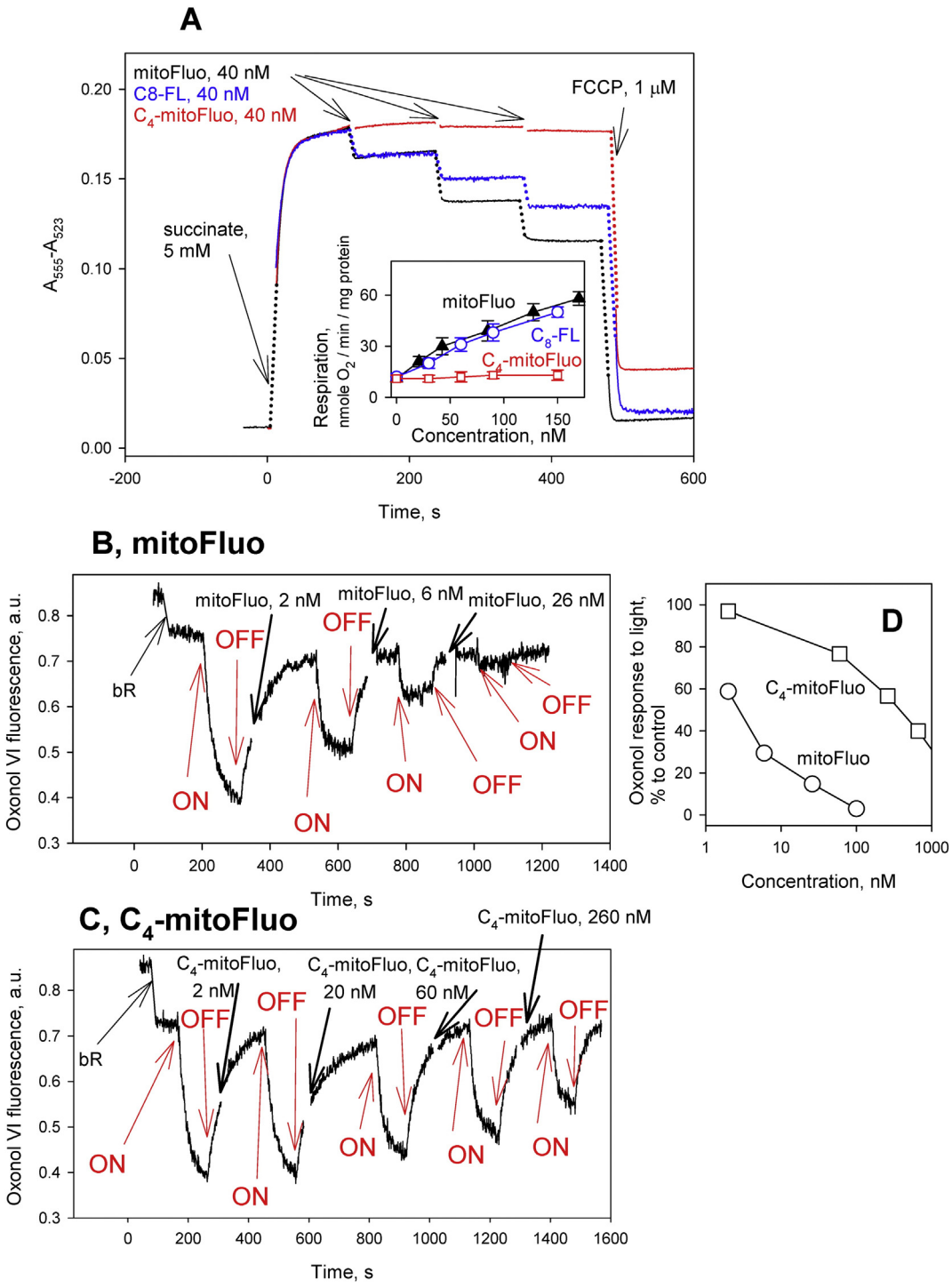

Fig. 2. A. Effect of mitoFluo, C_8-FL and C_4-mitoFluo on the membrane potential of rat liver mitochondria assessed by safranine O absorbance changes. Concentrations: safranine O, 15 μM; succinate, 5 mM; rotenone, 1 μM. For other conditions, see Materials and methods. Insert: Dependence of the mitochondrial respiration on the concentration of mitoFluo, C_8-FL and C_4-mitoFluo. **B–D**. Effect of mitoFluo and C_4-mitoFluo on the membrane potential of proteoliposomes with reconstituted bacteriorhodopsin assessed by oxonol VI fluorescence. Concentrations: oxonol VI, 10 μM; lipid, 100 μg/ml. For other conditions, see Materials and methods.

reduced upon the addition of 2 nM mitoFluo, but was practically unaltered at the same concentration of C_4-mitoFluo (Fig. 2C). The effective concentrations of the conjugates differed by about two orders of magnitude (panel D in Fig. 2). Interestingly, in bacteriorhodopsin proteoliposomes, mitoFluo appeared to be much more effective than FCCP, in contrast to the situation in mitochondria. In fact, about 100 nM of FCCP was required to reduce the oxonol VI response halftime (data not shown).

The striking difference in the behavior of mitoFluo and C_4-mitoFluo in the experiments depicted in Fig. 2 highlighted the role of the alkyl linker between the mitochondria-targeting TPP group and a proton-carrying moiety for uncoupling activity. The inactivity of MitoDNP as an uncoupler [27] was most likely also associated with the short (propyl) linker.

According to [10,43,44], the action of several popular uncouplers is mediated at least partially by their interaction with certain protein transporters located in the inner mitochondrial membrane. In particular, the action of DNP was partially inhibited by carboxyatractyloside (CAtr), a specific inhibitor of the ADP/ATP carrier [45], while the action of FCCP was blocked by 6-ketocholestanol [46,47]. It has been shown

Please cite this article as: Y.N. Antonenko, et al., A long-linker conjugate of fluorescein and triphenylphosphonium as mitochondria-targeted uncoupler and fluorescent neuro- and neph..., Biochim. Biophys. Acta (2016), http://dx.doi.org/10.1016/j.bbagen.2016.07.014

recently that the essential compound of the plant extract from *Verbesina persicifolia*, an eudesman derivative, uncouples mitochondria via interaction with the terminal proton pump cytochrome oxidase [48]. To gain insight into the possible interaction of mitoFluo with mitochondrial membrane proteins, we examined the sensitivity of its uncoupling activity to these recouplers. Neither 6-ketocholestanol nor CAtr inhibited the uncoupling action of mitoFluo or C_8-FL as judged from the membrane potential of rat liver mitochondria (black and blue curves in Fig. 3). Control experiments showed substantial sensitivity of FCCP action to 6-ketocholestanol and insensitivity to CAtr, while the opposite effects were observed with palmitate in agreement with the literature data (red and green curves in Fig. 3). These data pointed to the plain protonophoric activity of both mitoFluo and C_8-FL as a mechanism of their uncoupling action on mitochondria, although mitoFluo-mediated proton current across a planar BLM at neutral pH was substantially lower compared to that of C_8-FL [32,33].

To further examine the mechanism of the mitoFluo uncoupling action, we compared its protonophoric activity with that of C_4-mitoFluo by measuring proton diffusion potential on a planar BLM separating two solutions with different pH values. In such a system, the addition of a protonophore (e.g. FCCP) resulted in a transmembrane H^+ flux generating an electrical potential difference across the BLM, the more acidic compartment being negatively charged. It was found (Fig. 4) that mitoFluo (black curve), but not C_4-mitoFluo (red curve), effectively generated the proton diffusion potential. In the case of mitoFluo, the potential was close to the theoretical limit (about 60 mV), while in the case of C_4-mitoFluo, it was about three times lower, suggesting poor protonophoric activity exhibited by this short-linker analog in agreement with our uncoupling data in mitochondria (Fig. 2).

Fig. 1B shows a scheme of protonophoric action of mitoFluo on a lipid membrane. In contrast to other known protonophores (both anionic and cationic), two forms of mitoFluo responsible for proton transport are charged, one form being cationic, while another being zwitterionic. It is generally assumed that lipid membranes are impermeable for zwitterionic compounds, because even the presence of a single charge on a compound decreases its permeability by several orders of magnitude [49]. It has been shown, however, that the presence of an alkyl linker of the appropriate length makes TPP-based dications permeable through artificial lipid membranes and mitochondrial membranes [50,51]. Keeping in mind larger permeability of anions compared to cations of similar size due to the presence of the so-called dipole potential on the water-membrane interface of lipid membranes, it can be assumed that the permeability of the zwitterionic form of mitoFluo is not impossible. Of note, according to a recent study [49], the anticancer drug topotecan can permeate through lipid membranes in a zwitterionic form, showing the permeability close to that of the neutral form. Therefore, the scheme in Fig. 1B, which includes the step of the transmembrane diffusion of the zwitterionic form of mitoFluo, is justified and does not contradict the data available. This scheme assumes that the protonophoric action of mitoFluo proceeds predominately via shuttling from one membrane interface to the other rather than from one aqueous phase to the other. The poor activity of C_4-mitoFluo can be assigned to its weak lipophilicity preventing its binding to the membrane surface. An increase in the linker chain length by 6 carbon atoms should lead to about 1000-fold difference in the octanol-water partition coefficients [52,53].

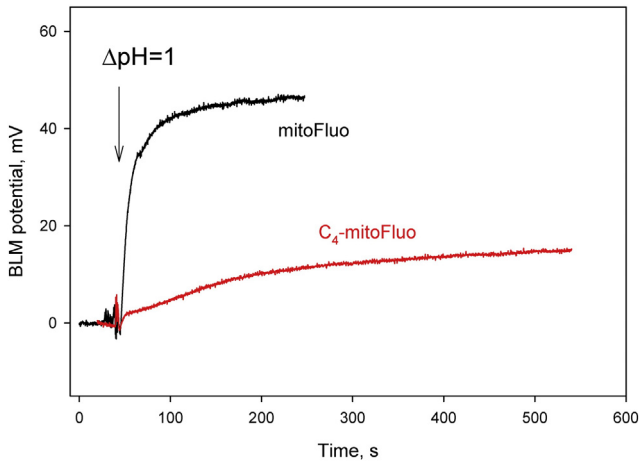

Fig. 4. MitoFluo was more effective than C_4-mitoFluo in the induction of H^+-diffusion potential on planar bilayer lipid membrane made from total lipid of *E. coli*. Concentrations of mitoFluo and C_4-mitoFluo were 0.25 μM. The solution was 10 mM MES, 10 mM β-alanine, 100 mM KCl, pH 4. Formation of ΔpH was performed by shifting pH to the value of 5 at one side of the BLM leading to positive potential at this side.

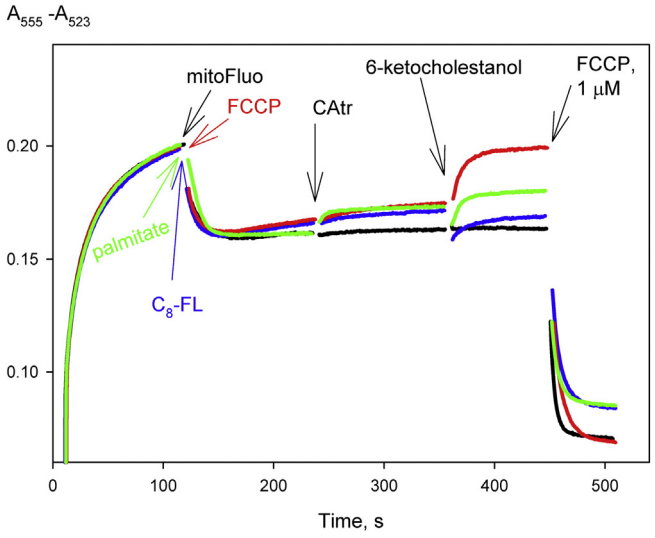

Fig. 3. Effect of 6-ketocholestanol (100 μM) and carboxyatractyloside (CAtr, 1 μM) on the uncoupling action of mitoFluo (black curve, 40 nM), C_8-FL (blue curve, 50 nM), FCCP (red curve, 20 nM), and palmitate (green curve, 15 μM) in rat liver mitochondria estimated by the mitochondrial membrane potential measurements with safranine O (15 μM). For other conditions, see Materials and methods.

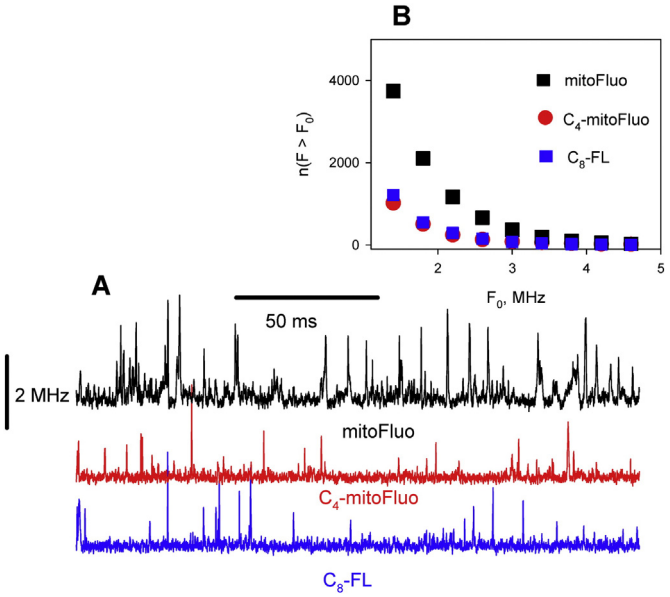

Fig. 5. Time-resolved count rates of 20 nM mitoFluo (black curve), 20 nM C_4-mitoFluo (red curve), and 20 nM C_8-FL (blue curve) in the presence of rat liver mitochondria (0.1 mg/ml) in the incubation buffer. The signal was recorded under stirring condition in solution: 250 mM sucrose, 20 mM MOPS, 1 mM EGTA, pH 7.4. **B.** Statistical analysis in the form of corresponding dependences of $n(F > F_0)$ on F_0 derived as described in the Materials and methods.

Please cite this article as: Y.N. Antonenko, et al., A long-linker conjugate of fluorescein and triphenylphosphonium as mitochondria-targeted uncoupler and fluorescent neuro- and neph..., Biochim. Biophys. Acta (2016), http://dx.doi.org/10.1016/j.bbagen.2016.07.014

To assess the role of the linker for mitochondrial targeting, we compared mitochondrial accumulation of mitoFluo and C_4-mitoFluo by the FCS technique, successfully used in our previous studies for TMRE and other rhodamine derivatives [38,54]. FCS is based on recording fluorescence fluctuations arising from the Brownian motion of single particles inside a small laser-illuminated volume (confocal volume) of about ~10^{-15} l [55]. The FCS recording obtained with C_4-mitoFluo (Fig. 5A, red curve) displayed only a small number of bright peaks, which corresponded to the passage of mitochondrial particles carrying C_4-mitoFluo across the confocal volume. In the case of mitoFluo, the number of the peaks was substantially higher (black curve in Fig. 5A, similar to the recording presented in [32]). These measurements were carried out in the presence of succinate, which provided generation of the mitochondrial membrane potential driving the permeating cations into mitochondria. The recording made in the presence of C_8-FL (Fig. 5A, blue curve) showed similar number of peaks as in the case of C_4-mitoFluo. The experimental data were obtained under stirring conditions which increased substantially the number of events, thereby enhancing the resolution of the method [38]. Panel B of Fig. 5 presented statistics of the number of peaks (n) with an amplitude exceeding the certain value F_0 (i.e. $n(F > F_0)$) during the recording of 30 s. The analysis confirmed our conclusion that the number of peaks in the case of mitoFluo was substantially higher than in the case of C_4-mitoFluo or C_8-FL (about 3–5 times depending on F_0). Therefore, C_4-mitoFluo accumulation in mitochondria (associated with its lower membrane permeability) was weaker than that of mitoFluo possibly because of its lower hydrophobicity. Limited accumulation of C_8-FL was in agreement with our previous measurements [33].

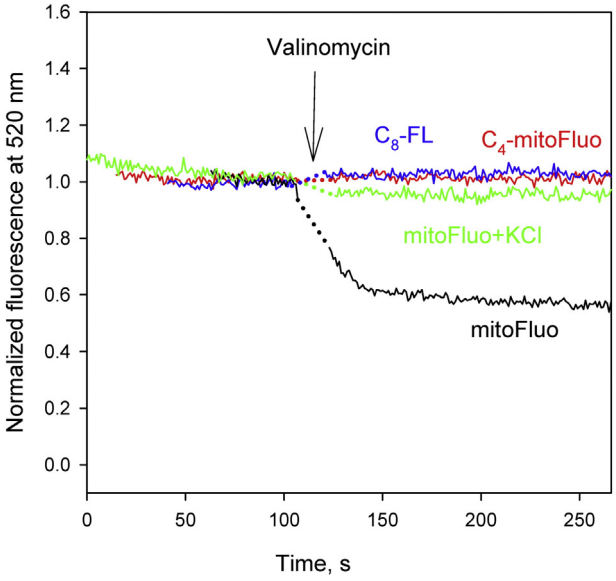

Fig. 7. Effect of K^+-diffusion potential in liposomes on the fluorescence of various fluorescein derivatives. Traces of fluorescence at 520 nm (excitation 490 nm) normalized to the signal prior to the addition of valinomycin are shown in a medium: 100 mM choline chloride, 3 mM Tris, pH 7.5. Additions: 10 nM valinomycin, 50 mM of KCl (green curve). Liposomes, 10 μg/ml DPhPC. Concentrations of mitoFluo, C_8-FL, and C_4-mitoFluo were 20 nM.

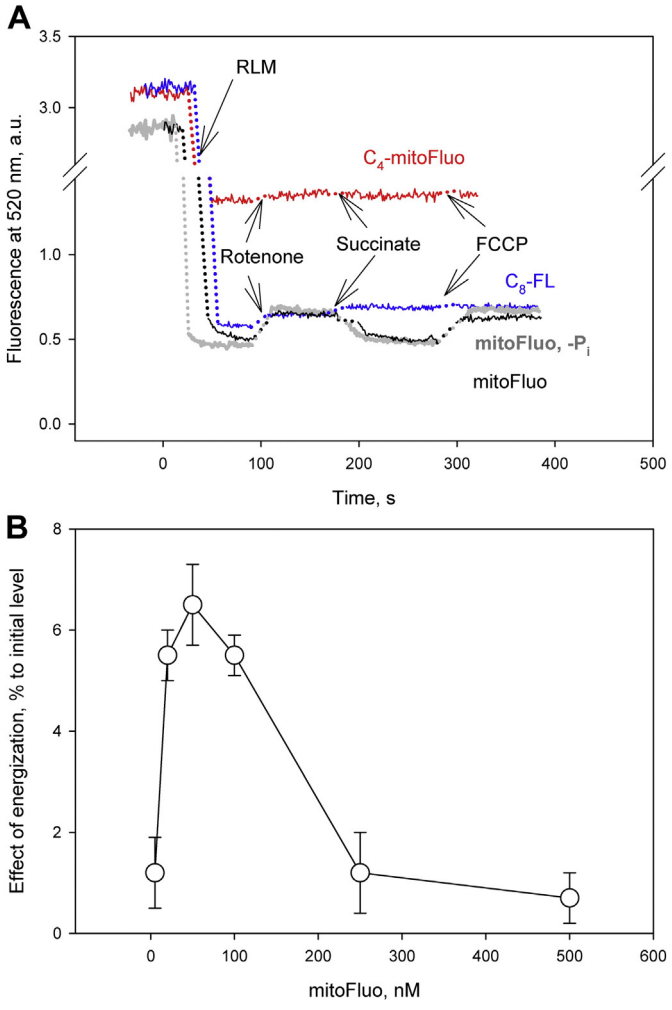

Fig. 6. A. Effect of mitochondrial energization on the fluorescence of different fluorescein derivatives. The fluorescence was normalized to the initial level measured prior to the addition of mitochondria. Traces of fluorescence at 520 nm (excitation 490 nm) are shown in a medium: 250 mM sucrose, 10 mM MOPS, 3 mM $MgCl_2$, 2 mM KH_2PO_4 (grey curve was without phosphate), 1 mM EGTA, pH 7.4. Additions where indicated: 0.2 mg/ml rat liver mitochondria (RLM), 1 μM rotenone, 5 mM succinate, 100 nM of FCCP. Concentrations of mitoFluo, C_8-FL, and C_4-mitoFluo were 20 nM. **B**. Dose dependence of the effect of succinate on the fluorescence of mitoFluo. Shown is the percent of the signal decrease with respect to the initial level of the mitoFluo fluorescence.

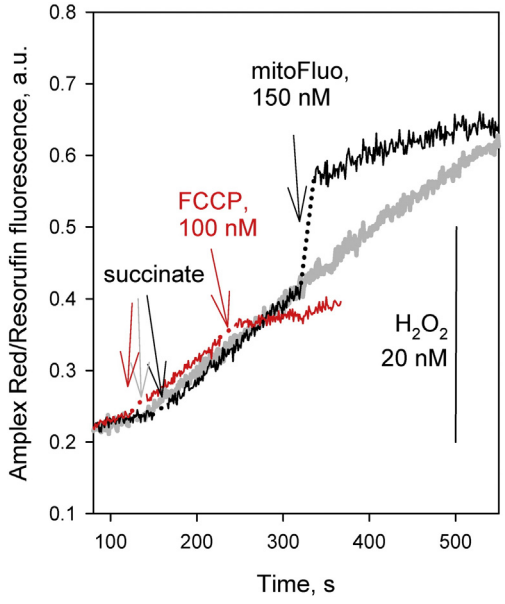

Fig. 8. Effect of mitoFluo (black curve) or FCCP (red curve) on H_2O_2 production in rat liver mitochondria. Incubation medium: 250 mM sucrose, 20 mM MOPS, 5 mM KH_2PO4, 3 mM $MgCl_2$, 1 mM EGTA, 1 μM Amplex Red, and 5 U/ml horseradish peroxidase, pH 7.4. Succinate, 3 mM, mitochondrial protein, 0.5 mg/ml.

Please cite this article as: Y.N. Antonenko, et al., A long-linker conjugate of fluorescein and triphenylphosphonium as mitochondria-targeted uncoupler and fluorescent neuro- and neph..., Biochim. Biophys. Acta (2016), http://dx.doi.org/10.1016/j.bbagen.2016.07.014

Fluorescence of mitoFluo in mitochondria could be sensitive to a mitochondrial functional state, because the fluorescence of fluorescein is strongly pH dependent (de-protonated form possesses bright fluorescence) and exhibits self-quenching. Energization of mitochondria should lead to an increase in the mitoFluo fluorescence due to alkalinization of the matrix pH. On the other hand, energization of mitochondria should decrease the mitoFluo fluorescence due to its accumulation inside the matrix resulting in an increase in its local concentration. Fig. 6A shows the time course of the mitoFluo fluorescence added to a suspension of rat liver mitochondria. Here, the concentration of mitoFluo (20 nM) was about an order of magnitude lower than its uncoupling concentrations (about 200 nM). The addition of rotenone increased the fluorescence signal, while succinate decreased the signal to the initial level, and subsequent addition of FCCP increased the signal up to the level observed with rotenone. It may be concluded that the changes in the mitoFluo fluorescence were reciprocal to corresponding changes in the mitochondrial membrane potential reported previously (see, for example, Fig. 9 in [56]), namely: mitochondria generated membrane potential, when respiring with endogenous substrates, rotenone depolarized the mitochondria by inhibiting respiratory complex I, the complex II substrate

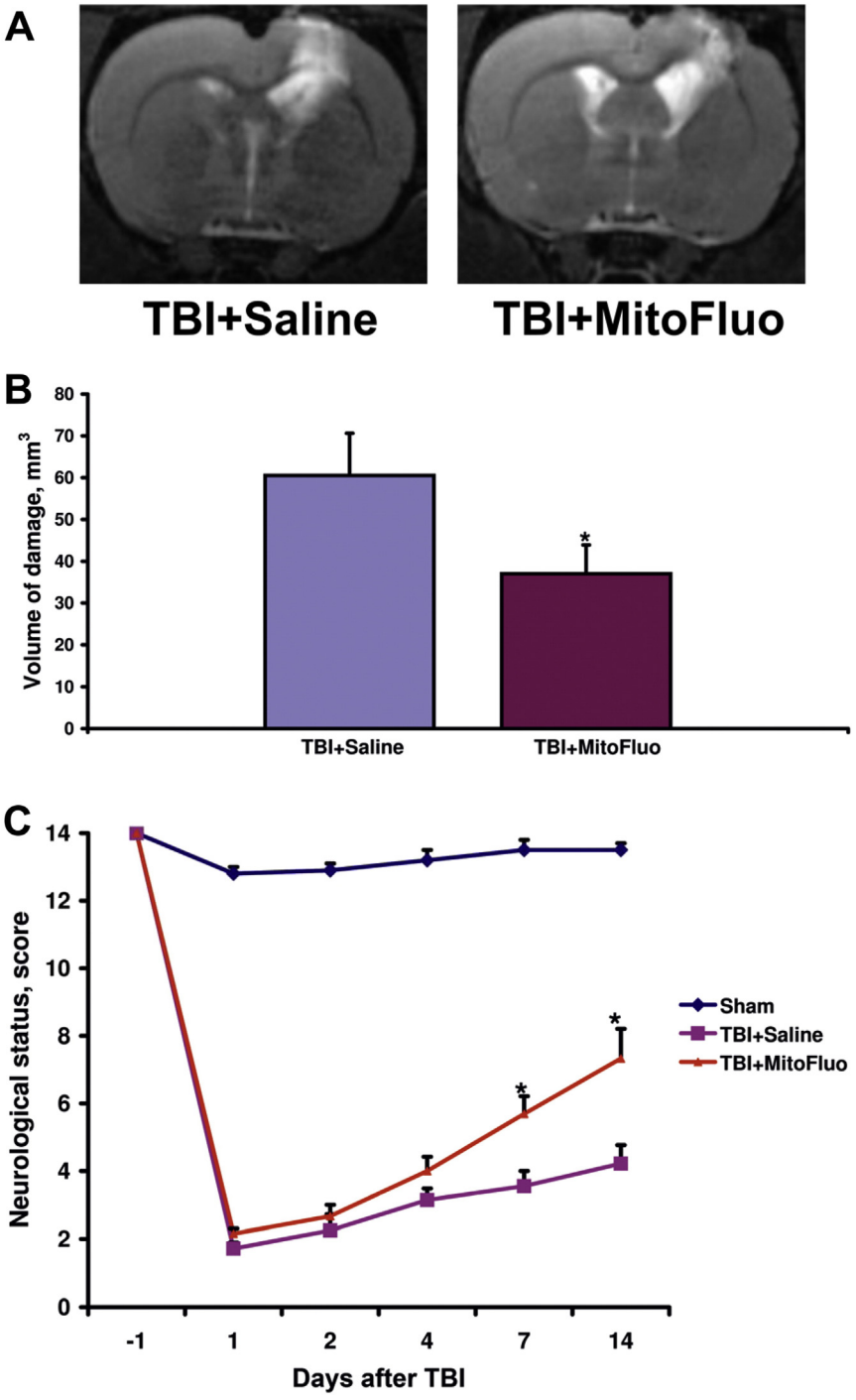

Fig. 9. Protection against traumatic brain injury by the mitoFluo treatment starting immediately after trauma. (A) Representative T2-weighted MR-images from coronal brain sections (0.8 mm thick, from rostral (top) towards caudal (bottom)) obtained on the 14th day after reperfusion. Light regions refer to ischemic areas. (B) Damage volume was evaluated by using MRI with analysis of T2-weighted images. (D) Neurological deficit scores estimated in the limb-placing test. *Denotes significant difference from the TBI + Saline or TBI + mitoFluo groups ($p < 0.05$) (One-way ANOVA, followed by Tukey's post-hoc analysis).

succinate restored the membrane potential, and the protonophore FCCP depolarized the mitochondria once again. With C_4-mitoFluo, the addition of mitochondria led to a substantially smaller decrease in the fluorescence, than with mitoFluo, and subsequent energization-deenergization did not change the level of the signal (Fig. 6A, red curve). The addition of 2 mM phosphate to the medium did not change the levels of the mitoFluo fluorescence before and after mitochondrial energization, suggesting that the alkalinization of the mitochondrial matrix upon energization did not contribute to changes in the mitoFluo fluorescence (Fig. 6A, grey curve). With C_8-FL lacking the TPP group, the fluorescence signal did not depend on the mitochondrial energization (Fig. 6A, blue curve), similar to the case of C_4-mitoFluo.

The decrease in the mitoFluo fluorescence upon mitochondrial energization could result from either a total increase of the protonation level of the compound or fluorescence self-quenching upon accumulation in the matrix. In view of the available data on the fluorescence behavior of a number of cationic dyes such as DiS-C3-(5) [57], safranine O [36], or TMRE [58], the self-quenching seems more justified. Consistent with this assumption, the degree of the mitoFluo quenching upon energization increased with raising mitoFluo concentration from 5 nM to 200 nM (Fig. 6B). Further elevation of the mitoFluo concentrations led to a relative decrease in the effect of energization due to the uncoupling action of mitoFluo.

We also tested potential-sensitive changes of mitoFluo fluorescence in a system of liposomes with the K^+ diffusion potential generated in the presence of valinomycin. It was shown previously that the fluorescence of cationic DiS-C3-(5) decreased in this system upon the addition of valinomycin due to concentration-dependent quenching of the dye [59]. Fig. 7 shows similar experiments with mitoFluo (black curve), C_4-mitoFluo (red curve) and C_8-FL (blue curve). In the case of mitoFluo,

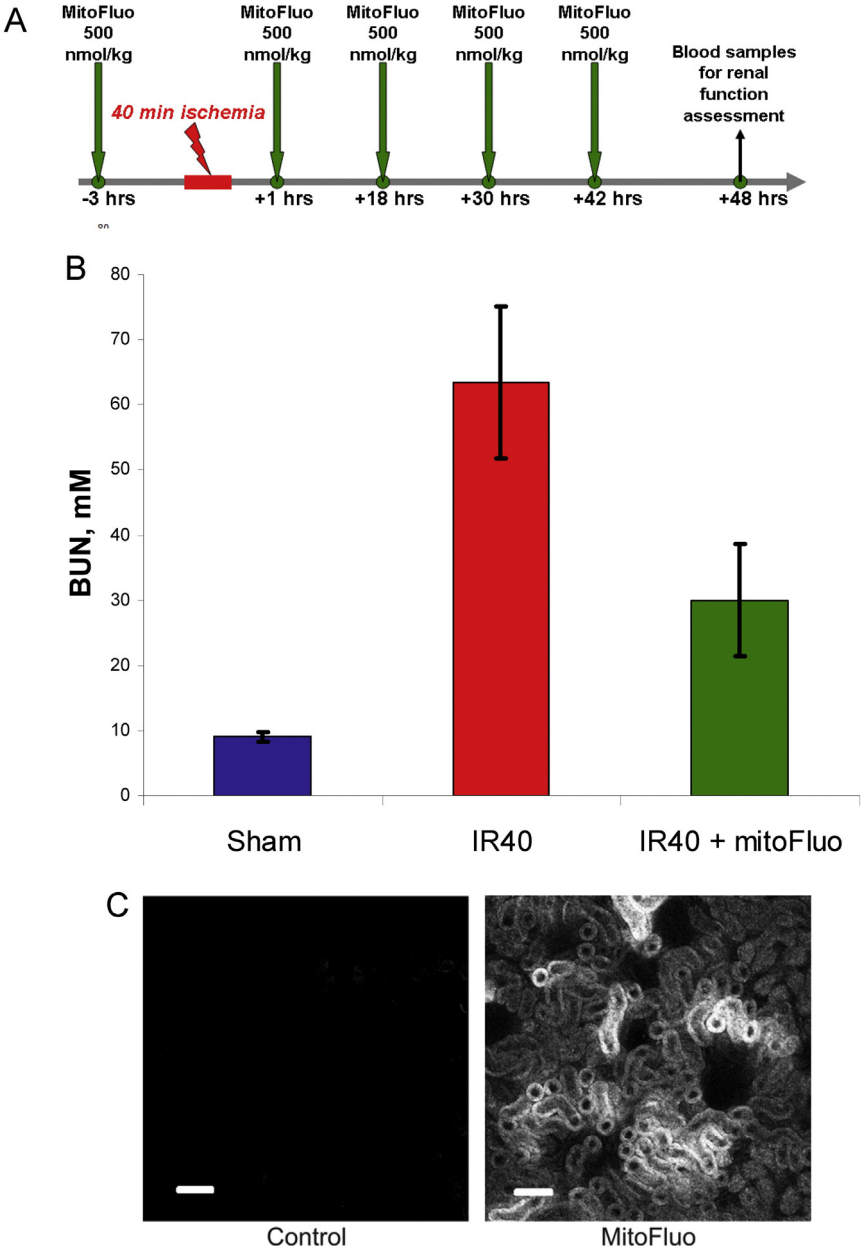

Fig. 10. MitoFluo prevents acute kidney injury after renal ischemia/reperfusion. A: Experimental design. Male rats were subjected to 40-min warm ischemia of the left kidney and right kidney nephrectomy. Blood samples were obtained 48 h after I/R to determine BUN. MitoFluo (500 nmoles/kg) was injected i/p 3 h before I/R, 1 h after I/R, and subsequent injections at 18, 30 and 42 h. B: Renal function estimated by BUN concentration 48 h after I/R. C: MitoFluo accumulates in kidney tubules after i/p injection. Confocal microscopy of kidney tissues slices 3 h after i/p injection of 2 μmol/kg mitoFluo showing its retention and distribution over kidney compartments (right panel). As a negative control, kidney from untreated animals was displayed (left panel). Bar, 100 μm.

Please cite this article as: Y.N. Antonenko, et al., A long-linker conjugate of fluorescein and triphenylphosphonium as mitochondria-targeted uncoupler and fluorescent neuro- and neph..., Biochim. Biophys. Acta (2016), http://dx.doi.org/10.1016/j.bbagen.2016.07.014

the addition of valinomycin (at t = 110 s) led to a decrease in the fluorescence signal (about 50%, black curve), while there was no fluorescence decrease in the absence of the K^+ gradient on liposomes (about 5%, green curve). In agreement with the data on mitochondria, fluorescence of C_4-mitoFluo and C_8-FL did not respond to changes in membrane potential of liposomes (red and blue curves in Fig. 7). Based on these results, mitoFluo might be proposed as the mitochondrial membrane potential fluorescent probe in a certain concentration range. However, strong energy-independent binding, the narrow dynamic range and confounding uncoupling properties make it rather unsuitable.

As it was pointed out in the Introduction, uncouplers exhibited protective action in several pathologies, associated with the oxidative stress, possibly as a result of their ability to reduce ROS generation by mitochondria [5,60]. However, this phenomenon was shown for classical anionic uncouplers which may act by the mechanism differing from that of mitoFluo. To this end, we measured the effect of mitoFluo on the generation of hydrogen peroxide by mitochondria using an Amplex Red/HRP system. Fig. 8 demonstrates that mitoFluo decreased the H_2O_2 production of rat liver mitochondria in the presence of succinate as a substrate. Grey curve is a recording of H_2O_2 production during 10 min, red curve displays an experiment with FCCP. Black curve shows that the addition of 150 nM mitoFluo led to a jump of the fluorescence, measured at 620 nm, due to fluorescent properties of mitoFluo, however the slope of the curve after the addition of mitoFluo was substantially smaller, thereby demonstrating the suppressed rate of H_2O_2 production, as measured by fluorescence of the Amplex Red oxidation product resorufin. Thus, mitoFluo could be used as an inhibitor of ROS production similar to other anionic uncouplers.

Keeping in mind neuroprotective properties of uncouplers in stroke [30,61,62] or in brain trauma models [63,64], we examined the protective effects of intranasal (i/n) instillation of mitoFluo on a traumatic brain injury (TBI) model in rats, if mitoFluo was administered immediately after trauma. In our experiments TBI caused an extensive damage of sensorimotor cortex (Fig. 9A). When compared with the control group, the treatment with mitoFluo at doses 500 nmol/kg reduced the damage volume by 40% ($p < 0.05$, Fig. 9B). The results of the limb-placing test revealed the development of a post-traumatic functional deficit in the right limbs, whereas it was absent in the left limbs. Before the induction of trauma, the intact rats scored 14.0 ± 0 in limb-placing test, and sham-operated animals scored 12.8 ± 0.2, while on the first day after TBI rats scored only 1.7 ± 0.2. The treatment with mitoFluo restored the neurological status to 5.7 ± 0.5 and 7.3 ± 0.9 scores ($p < 0.05$) on the 7th and the 14th day after TBI, while TBI + Saline group scored 3.6 ± 0.4 and 4.2 ± 0.5, respectively (Fig. 9C).

We also performed other series of experiments on rats using a model of kidney ischemia/reperfusion (I/R). Animals, that underwent right nephrectomy, exhibited a dramatic rise in BUN on the second day after I/R (Fig. 10A,B). The treatment with mitoFluo (i/p injection of 500 nmoles/kg) prior to ischemia and during the reperfusion phase significantly lowered BUN, thereby showing diminished acute renal damage (Fig. 10B). We analyzed accumulation of mitoFluo in kidney by fluorescence distribution using tissue sections sampled 3 h after i/p injection of mitoFluo to a rat in the dose of 2 μmol/kg. We found that fluorescence of mitoFluo was visible in the kidney 3 h after injection (Fig. 10C) and remained detectable up to 24 h after injection (data not shown). The fluorescence was clearly seen in kidney tubular epithelial cells but not in glomeruli.

Previous studies have revealed an apparent neuroprotective effect of uncouplers of oxidative phosphorylation in stroke and traumatic models [30,61–64], along with nephroprotective and cardioprotective action [5]. These effects have been interpreted in terms of modulation of ROS production by the mitochondrial membrane potential yielding an obviously dangerous elevated production of ROS at high potentials as a result of excessive reduction of auto-oxidizable components of the mitochondrial respiratory chain [9]. In this context, lowering the membrane potential would diminish the probability of an electron leak to molecular oxygen, thereby leading to a drop of mitochondrial ROS production to a more safe level. According to our data (Fig. 8), mitoFluo exhibited this ability in isolated mitochondria. This consideration explains mitoFluo action both in brain trauma model (Fig. 9) and the kidney ischemia/reperfusion model (Fig. 10). Importantly, the uncoupling concentration of mitoFluo in different tissues in vivo was lower than its cytotoxic concentration: in particular, the IC50 of mitoFluo in cells of transformed fibroblasts was found to be 2 μM [32]. Thus, our in vivo data showed the therapeutic potential of mitoFluo as a neuroprotector and a nephroprotector. We believe that the tissue protection experiments (Figs. 9, 10) can be considered as a proof of concept experiments for mitochondria-targeted uncouplers and further work is required to develop an uncoupler exhibiting maximum protection with minimum side-effect properties. Further optimization of the linker chain length is in progress, while the choice of fluorescein as a protonophoric unit is under consideration.

Transparency document

The Transparency document associated with this article can be found, in online version.

Acknowledgements

The authors are grateful to Professor Vladimir Skulachev for valuable discussions. This work was financially supported by the Russian Science Foundation grant 16-14-10025.

References

[1] J.A. Harper, K. Dickinson, M.D. Brand, Mitochondrial uncoupling as a target for drug development for the treatment of obesity, Obes. Rev. 2 (2001) 255–265.
[2] R.J. Perry, D.Y. Zhang, X.M. Zhang, J.L. Boyer, G.I. Shulman, Controlled-release mitochondrial protonophore reverses diabetes and steatohepatitis in rats, Science 347 (2015) 1253–1256.
[3] M. Goldgof, C.Y. Xiao, T. Chanturiya, W. Jou, O. Gavrilova, M.L. Reitman, The Chemical Uncoupler 2,4-dinitrophenol (DNP) protects against diet-induced obesity and improves energy homeostasis in mice at thermoneutrality, J. Biol. Chem. 289 (2014) 19341–19350.
[4] H.L. Tao, Y. Zhang, X.G. Zeng, G.I. Shulman, S.K. Jin, Niclosamide ethanolamine-induced mild mitochondrial uncoupling improves diabetic symptoms in mice, Nat. Med. 20 (2014) 1263–1269.
[5] Cunha, F. M., Caldeira da Silva, C. C., Cerqueira, F. M., Kowaltowski, A. J. Mild mitochondrial uncoupling as a therapeutic strategy. Curr. Drug Targets 12 (2011), 783–789.
[6] R.A.Smith, M.P.Murphy, Animal and human studies with the mitochondria-targeted antioxidant MitoQ, Ann. N. Y. Acad. Sci. 1201 (2010) 96–103.
[7] R. Wen, B. Banik, R.K. Pathak, A. Kumar, N. Kolishetti, S. Dhar, Nanotechnology inspired tools for mitochondrial dysfunction related diseases, Adv. Drug Deliv. Rev. 99 (2016) 52–69.
[8] S.I. Dikalov, A.E. Dikalova, Contribution of mitochondrial oxidative stress to hypertension, Curr. Opin. Nephrol. Hypertens. 25 (2016) 73–80.
[9] S.S. Korshunov, V.P. Skulachev, A.A. Starkov, High protonic potential actuates a mechanism of production of reactive oxygen species in mitochondria, FEBS Lett. 416 (1997) 15–18.
[10] V.P. Skulachev, Uncoupling: new approaches to an old problem of bioenergetics, Biochim. Biophys. Acta 1363 (1998) 100–124.
[11] E. Klotzsch, A. Smorodchenko, L. Lofler, R. Moldzio, E. Parkinson, G.J. Schutz, E.E. Pohl, Superresolution microscopy reveals spatial separation of UCP4 and F0F1-ATP synthase in neuronal mitochondria, Proc. Natl. Acad. Sci. U. S. A. 112 (2015) 130–135.
[12] A. Rupprecht, E.A. Sokolenko, V. Beck, O. Ninnemann, M. Jaburek, T. Trimbuch, S.S. Klishin, P. Jezek, V.P. Skulachev, E.E. Pohl, Role of the transmembrane potential in the membrane proton leak, Biophys. J. 98 (2010) 1503–1511.
[13] J. Ilivicky, J.E. Casida, Uncoupling action of 2,4-dinitrophenols, 2-trifluoromethylbenzimidazoles and certain other pesticide chemicals upon mitochondria from different sources and its relation to toxicity, Biochem. Pharmacol. 18 (1969) 1389–1401.
[14] X.X. Feng, W. Zhu, L.A. Schurig-Briccio, S. Lindert, C. Shoen, R. Hitchings, J.K. Li, Y. Wang, N. Baig, T.H. Zhou, B.K. Kim, D.C. Crick, M. Cynamon, J.A. McCammon, R.B. Gennis, E. Oldfield, Antiinfectives targeting enzymes and the proton motive force, Proc. Natl. Acad. Sci. U. S. A. 112 (2015) E7073–E7082.
[15] E. Colman, Dinitrophenol and obesity: an early twentieth-century regulatory dilemma, Regul. Toxicol. Pharmacol. 48 (2007) 115–117.
[16] P.H. Lou, B.S. Hansen, P.H. Olsen, S. Tullin, M.P. Murphy, M.D. Brand, Mitochondrial uncouplers with an extraordinary dynamic range, Biochem. J. 407 (2007) 129–140.
[17] K. Ingolfsdottir, Usnic acid, Phytochemistry 61 (2002) 729–736.

[18] Y.R. Krishna, V. Mittal, P. Grewal, M. Fiel, T. Schiano, Acute liver failure caused by 'fat burners' and dietary supplements: A case report and literature review, Can. J. Gastroenterol. Hepatol. 25 (2011) 157–160.

[19] Y.N. Antonenko, L.S. Khailova, D.A. Knorre, O.V. Markova, T.I. Rokitskaya, T.M. Ilyasova, I.I. Severina, E.A. Kotova, Y.E. Karavaeva, A.S. Prikhodko, F.F. Severin, V.P. Skulachev, Penetrating cations enhance uncoupling activity of anionic protonophores in mitochondria, PLoS One 8 (2013), e61902.

[20] D.G. Nicholls, Simultaneous monitoring of ionophore- and inhibitor-mediated plasma and mitochondrial membrane potential changes in cultured neurons, J. Biol. Chem. 281 (2006) 14864–14874.

[21] B.M. Kenwood, J.L. Weaver, A. Bajwa, I.K. Poon, F.L. Byrne, B.A. Murrow, J.A. Calderone, L. Huang, A.S. Divakaruni, J.L. Tomsig, K. Okabe, R.H. Lo, C.G. Cameron, L. Columbus, Z. Yan, J.J. Saucerman, J.S. Smith, J.W. Holmes, K.R. Lynch, K.S. Ravichandran, S. Uchiyama, W.L. Santos, G.W. Rogers, M.D. Okusa, D.A. Bayliss, K.L. Hoehn, Identification of a novel mitochondrial uncoupler that does not depolarize the plasma membrane, Mol. Metab. 3 (2014) 114–123.

[22] J. Wolff, M.E. Standaert, J.E. Rall, Thyroxine displacement from serum proteins and depression of serum protein-bound iodine by certain drugs, J. Clin. Invest. 40 (1961) 1373–1379.

[23] C. Osorio, Effect of salicylate and dinitrophenol on binding of thyroid hormones by human and rat serum proteins at pH 7.4, J. Physiol. 163 (1962) 151–159.

[24] L. Drobnica, E. Sturdik, Reaction of carbonyl cyanide phenylhydrazones with thiols, Biochim. Biophys. Acta 585 (1979) 462–476.

[25] H. Hayashi, G.A. Plishker, J.T. Penniston, Effect of carbonylcyanide *m*-chlorophenylhydrazone on calcium-stimulated ATPase activity of erythrocyte ghosts, Biochim. Biophys. Acta 394 (1975) 145–155.

[26] R.J. Perry, T. Kim, X.M. Zhang, H.Y. Lee, D. Pesta, V.B. Popov, D.Y. Zhang, Y. Rahimi, M.J. Jurczak, G.W. Cline, D.A. Spiegel, G.I. Shulman, Reversal of hypertriglyceridemia, fatty liver disease, and insulin resistance by a liver-targeted mitochondrial uncoupler, Cell Metab. 18 (2013) 740–748.

[27] F.H. Blaikie, S.E. Brown, L.M. Samuelsson, M.D. Brand, R.A. Smith, M.P. Murphy, Targeting dinitrophenol to mitochondria: limitations to the development of a self-limiting mitochondrial protonophore, Biosci. Rep. 26 (2006) 231–243.

[28] L. Biasutto, N. Sassi, A. Mattarei, E. Marotta, P. Cattelan, A. Toninello, S. Garbisa, M. Zoratti, C. Paradisi, Impact of mitochondriotropic quercetin derivatives on mitochondria, Biochim. Biophys. Acta Bioenerg. 1797 (2010) 189–196.

[29] Y.N. Antonenko, A.V. Avetisyan, D.A. Cherepanov, D.A. Knorre, G.A. Korshunova, O.V. Markova, S.M. Ojovan, I.V. Perevoshchikova, A.V. Pustovidko, T.I. Rokitskaya, I.I. Severina, R.A. Simonyan, E.A. Smirnova, A.A. Sobko, N.V. Sumbatyan, F.F. Severin, V.P. Skulachev, Derivatives of rhodamine 19 as mild mitochondria-targeted cationic uncouplers, J. Biol. Chem. 286 (2011) 17831–17840.

[30] L.S. Khailova, D.N. Silachev, T.I. Rokitskaya, A.V. Avetisyan, K.G. Lyamsaev, I.I. Severina, T.M. Il'yasova, M.V. Gulyaev, V.I. Dedukhova, T.A. Trendeleva, E.Y. Plotnikov, R.A. Zvyagilskaya, B.V. Chernyak, D.B. Zorov, Y.N. Antonenko, V.P. Skulachev, A short-chain alkyl derivative of Rhodamine 19 acts as a mild uncoupler of mitochondria and a neuroprotector, Biochim. Biophys. Acta Bioenerg. 1837 (2014) 1739–1747.

[31] A.V. Kalinovich, I.G. Shabalina, Novel mitochondrial cationic uncoupler C(4)R1 is an effective treatment for combating obesity in mice, Biochemistry (Mosc) 80 (2015) 620–628.

[32] S.S. Denisov, E.A. Kotova, E.Y. Plotnikov, A.A. Tikhonov, D.B. Zorov, G.A. Korshunova, Y.N. Antonenko, A mitochondria-targeted protonophoric uncoupler derived from fluorescein, Chem. Commun. 50 (2014) 15366–15369.

[33] M.M. Shchepinova, S.S. Denisov, E.A. Kotova, L.S. Khailova, D.A. Knorre, G.A. Korshunova, V.N. Tashlitsky, F.F. Severin, Y.N. Antonenko, Dodecyl and octyl esters of fluorescein as protonophores and uncouplers of oxidative phosphorylation in mitochondria at submicromolar concentrations, Biochim. Biophys. Acta Bioenerg. 1837 (2014) 149–158.

[34] K.S. Huang, H. Bayley, H.G. Khorana, Delipidation of bacteriorhodopsin and reconstitution with exogenous phospholipid, Proc. Natl. Acad. Sci. U. S. A. 77 (1980) 323–327.

[35] D. Johnson, H. Lardy, Isolation of liver or kidney mitochondria, Methods Enzymol. 10 (1967) 94–96.

[36] K.E. Akerman, M.K. Wikstrom, Safranine as a probe of the mitochondrial membrane potential, FEBS Lett. 68 (1976) 191–197.

[37] A.A. Starkov, G. Fiskum, Regulation of brain mitochondrial H_2O_2 production by membrane potential and NAD(P)H redox state, J. Neurochem. 86 (2003) 1101–1107.

[38] I.V. Perevoshchikova, D.B. Zorov, Y.N. Antonenko, Peak intensity analysis as a method for estimation of fluorescent probe binding to artificial and natural nanoparticles: tetramethylrhodamine uptake by isolated mitochondria, Biochim. Biophys. Acta Biomembr. 1778 (2008) 2182–2190.

[39] D.M.Feeney, M.G.Boyeson, R.T.Linn, H.M.Murray, W.G.Dail, Responses to cortical injury. 1. Methodology and local effects of contusions in the rat, Brain Res. 211 (1981) 67–77.

[40] N.K. Isaev, S.V. Novikova, E.V. Stelmashook, I.V. Barskov, D.N. Silachev, L.G. Khaspekov, V.P. Skulachev, D.B. Zorov, Mitochondria-targeted plastoquinone antioxidant SkQR1 decreases trauma-induced neurological deficit in rat, Biochemistry (Mosc) 77 (2012) 996–999.

[41] D.N. Silachev, A.A. Uchevatkin, Y.A. Pirogov, D.B. Zorov, N.K. Isaev, Comparative evaluation of two methods for studies of experimental focal ischemia: magnetic resonance tomography and triphenyltetrazoleum detection of brain injuries, Bull. Exp. Biol. Med. 147 (2009) 269–272.

[42] J. Jolkkonen, K. Puurunen, S. Rantakomi, A. Harkonen, A. Haapalinna, J. Sivenius, Behavioral effects of the alpha-adrenoceptor antagonist, atipamezole, after focal cerebral ischemia in rats, Eur. J. Pharmacol. 400 (2000) 211–219.

[43] A.A. Starkov, "mild" uncoupling of mitochondria, Biosci. Rep. 17 (1997) 273–279.

[44] A.A. Starkov, Protein-mediated energy-dissipating pathways in mitochondria, Chem. Biol. Interact. 163 (2006) 133–144.

[45] A.Y. Andreyev, T.O. Bondareva, V.I. Dedukhova, E.N. Mokhova, V.P. Skulachev, L.M. Tsofina, N.I. Volkov, T.V. Vygodina, The ATP/ADP-antiporter is involved in the uncoupling effect of fatty acids on mitochondria, Eur. J. Biochem. 182 (1989) 585–592.

[46] A.A. Starkov, V.I. Dedukhova, V.P. Skulachev, 6-ketocholestanol abolishes the effect of the most potent uncouplers of oxidative phosphorylation in mitochondria, FEBS Lett. 355 (1994) 305–308.

[47] J.L. Figarola, J. Singhal, J.D. Tompkins, G.W. Rogers, C. Warden, D. Horne, A.D. Riggs, S. Awasthi, S.S. Singhal, SR4 uncouples mitochondrial oxidative phosphorylation, modulates AMP-dependent kinase (AMPK)-mammalian target of rapamycin (mTOR) signaling, and inhibits proliferation of HepG2 hepatocarcinoma cells, J. Biol. Chem. 290 (2015) 30321–30341.

[48] V.L.Dalla, A.N.Garcia-Argaez, A.Braga, M.Martinez-Vazquez, S.Grancara, P.Martinis, E.Agostinelli, A.Toninello, An eudesman derivative from *Verbesina persicifolia D.C.* as a natural mild uncoupler in liver mitochondria. A new potential anti-obesity agent? Curr. Pharm. Des. 20 (2014) 253–261.

[49] K.D. Fugit, B.D. Anderson, The role of pH and ring-opening hydrolysis kinetics on liposomal release of topotecan, J. Control. Release 174 (2014) 88–97.

[50] M.F. Ross, T. Da Ros, F.H. Blaikie, T.A. Prime, C.M. Porteous, I.I. Severina, V.P. Skulachev, H.G. Kjaergaard, R.A. Smith, M.P. Murphy, Accumulation of lipophilic dications by mitochondria and cells, Biochem. J. 400 (2006) 199–208.

[51] I.I. Severina, M.Y. Vyssokikh, A.V. Pustovidko, R.A. Simonyan, T.I. Rokitskaya, V.P. Skulachev, Effects of lipophilic dications on planar bilayer phospholipid membrane and mitochondria, Biochim. Biophys. Acta Bioenerg. 1767 (2007) 1164–1168.

[52] A. Leo, C. Hansch, D. Elkins, Partition coefficients and their uses, Chem. Rev. 71 (1971) 525–616.

[53] J. Asin-Cayuela, A.R. Manas, A.M. James, R.A. Smith, M.P. Murphy, Fine-tuning the hydrophobicity of a mitochondria-targeted antioxidant, FEBS Lett. 571 (2004) 9–16.

[54] Y.N. Antonenko, I.V. Perevoshchikova, T.I. Rokitskaya, R.A. Simonyan, V.V. Tashlitsky, V.P. Skulachev, Effect of liposomes on energy-dependent uptake of the antioxidant SkQR1 by isolated mitochondria, J. Bioenerg. Biomembr. 44 (2012) 453–460.

[55] S.T. Hess, S. Huang, A.A. Heikal, W.W. Webb, Biological and chemical applications of fluorescence correlation spectroscopy: a review, Biochemistry 41 (2002) 697–705.

[56] Y.N. Antonenko, T.I. Rokitskaya, A. Huczynski, Electrogenic and nonelectrogenic ion fluxes across lipid and mitochondrial membranes mediated by monensin and monensin ethyl ester, Biochim. Biophys. Acta Biomembr. 1848 (2015) 995–1004.

[57] P.C. Laris, D.P. Bahr, R.R. Chaffee, Membrane potentials in mitochondrial preparations as measured by means of a cyanine dye, Biochim. Biophys. Acta 376 (1975) 415–425.

[58] R.C. Scaduto, L.W. Grotyohann, Measurement of mitochondrial membrane potential using fluorescent rhodamine derivatives, Biophys. J. 76 (1999) 469–477.

[59] T. Konishi, N. Murakami, Y. Hatano, K. Nakazato, Simultaneous determination of membrane-potential and pH gradient by photodiode array spectroscopy, Biochim. Biophys. Acta 862 (1986) 278–284.

[60] V.P. Skulachev, Y.N. Antonenko, D.A. Cherepanov, B.V. Chernyak, D.S. Izyumov, L.S. Khailova, S.S. Klishin, G.A. Korshunova, K.G. Lyamzaev, O.Y. Pletjushkina, V.A. Roginsky, T.I. Rokitskaya, F.F. Severin, I.I. Severina, R.A. Simonyan, M.V. Skulachev, N.V. Sumbatyan, E.I. Sukhanova, V.N. Tashlitsky, T.A. Trendeleva, M.Y. Vyssokikh, R.A. Zvyagilskaya, Prevention of cardiolipin oxidation and fatty acid cycling as two antioxidant mechanisms of cationic derivatives of plastoquinone (SkQs), Biochim. Biophys. Acta Bioenerg. 1797 (2010) 878–889.

[61] A.S. Korde, P.G. Sullivan, W.F. Maragos, The uncoupling agent 2,4-dinitrophenol improves mitochondrial homeostasis following striatal quinolinic acid injections, J. Neurotrauma 22 (2005) 1142–1149.

[62] D.N. Silachev, L.S. Khailova, V.A. Babenko, M.V. Gulyaev, S.I. Kovalchuk, L.D. Zorova, E.Y. Plotnikov, Y.N. Antonenko, D.B. Zorov, Neuroprotective effect of glutamate-substituted analog of gramicidin A is mediated by the uncoupling of mitochondria, Biochim. Biophys. Acta, Gen. Subj. 1840 (2014) 3434–3442.

[63] J.D. Pandya, J.R. Pauly, V.N. Nukala, A.H. Sebastian, K.M. Day, A.S. Korde, W.F. Maragos, E.D. Hall, P.G. Sullivan, Post-injury administration of mitochondrial uncouplers increases tissue sparing and improves behavioral outcome following traumatic brain injury in rodents, J. Neurotrauma 24 (2007) 798–811.

[64] J.D. Pandya, J.R. Pauly, P.G. Sullivan, The optimal dosage and window of opportunity to maintain mitochondrial homeostasis following traumatic brain injury using the uncoupler FCCP, Exp. Neurol. 218 (2009) 381–389.

Please cite this article as: Y.N. Antonenko, et al., A long-linker conjugate of fluorescein and triphenylphosphonium as mitochondria-targeted uncoupler and fluorescent neuro- and neph..., Biochim. Biophys. Acta (2016), http://dx.doi.org/10.1016/j.bbagen.2016.07.014